

PAPER • OPEN ACCESS

## Ultrashort pulse decomposition in reflection symmetric meander lines of three cascaded half-turns

To cite this article: E B Chernikova *et al* 2019 *J. Phys.: Conf. Ser.* **1353** 012024

View the [article online](#) for updates and enhancements.



**IOP | ebooks™**

Bringing you innovative digital publishing with leading voices to create your essential collection of books in STEM research.

Start exploring the collection - download the first chapter of every title for free.

# Ultrashort pulse decomposition in reflection symmetric meander lines of three cascaded half-turns

**E B Chernikova, A O Belousov and T R Gazizov**

Tomsk State University of Control Systems and Radioelectronics, 40, Lenina ave.,  
Tomsk, 634050, Russia

E-mail: [chiernikova96@mail.ru](mailto:chiernikova96@mail.ru)

**Abstract.** For the first time the quasi-static simulation of the time response of three cascaded half-turns of a reflection symmetric meander line to the excitation of an ultrashort pulse (USP) is performed. It is shown that the output voltage amplitude is determined by the amplitude of the first group of pulses. The possibility of additional pulses in the output signal is revealed. The simulation revealed the possibility of additional pulses at the output signal whose delays are equal to the arithmetic mean values of the pulse delays. The results of the work are useful for improving USP protection devices, inasmuch as the presence of additional pulses opens up further possibilities for more efficient use of such devices as this provides increased attenuation.

## 1. Introduction

Radio-electronic equipment (REE) is an integral part of human life. Since the failure of the REE (especially critical) can lead to various negative consequences, it is important to protect it [1]. A common reason for REE malfunctioning can be conducted interference, which can penetrate into REE directly through the conductors [2]. A typical example of such excitation is an ultrashort pulse (USP) [3], which, due to ultra-wideband spectrum, is able to penetrate into REE and, due to high power, disable it.

Protection devices connected to the equipment input have a number of disadvantages (low power, insufficient operating speed, spurious parameters and short service life) that make it difficult to protect equipment against powerful USPs. Besides, practical application also requires simplicity and cheapness, therefore, a search for new principles for improving the protection of REE against USPs is necessary. One of such principles is modal filtration, which implies the decomposition of a USP into pulses of lower amplitude due to differences in mode delays. This is implemented through the use of appropriate protection devices: modal filters (MF) and meander lines (ML). Meanwhile, a hybrid performance of such devices has not been previously considered, although this is relevant.

In addition, a new approach to improve modal filtration using a reflection symmetric MF is proposed (Figure 1). It is noteworthy since by providing both the edge and broad-side couplings between the conductors at certain parameters it allows obtaining USP decomposition pulses at the line output with nearly equal values of the pulse amplitudes and the time intervals between the pulses (Figure 1).



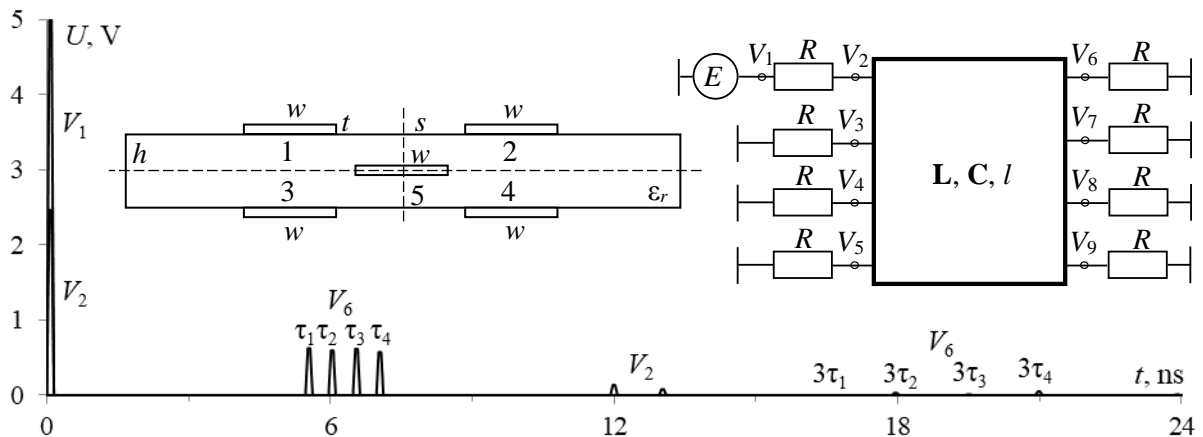


**Figure 1.** Schematic diagram, cross section and waveforms of EMF ( $V_1$ ), input ( $V_2$ ) and output ( $V_6$ ) voltages of a reflection symmetric MF.

The analysis of the reflection symmetric MF diagram shows the possibility of connecting half-turns with bridges in the form of an ML. Earlier [5], the configuration of a reflection symmetric ML of 4 cascaded half-turns has been considered, where the signal passes the maximum path (from the generator to the load) for a length of  $4l$ . Meanwhile, the analysis of the reflection symmetric MF connection diagram allows us to identify other options for connecting half-turns. A logical continuation of the reflection symmetric ML research is a diagram in which the signal propagates a length of  $3l$  from the generator to the load, i.e. along 3 cascaded half-turns with resistors connected to the ends of the fourth conductor. The aim of this work is to investigate the possibility to decompose a USP in such structures.

### 2. Structures under investigation

As a result, we obtained 3 diagrams giving different waveforms of voltage at the output (Figure 2).

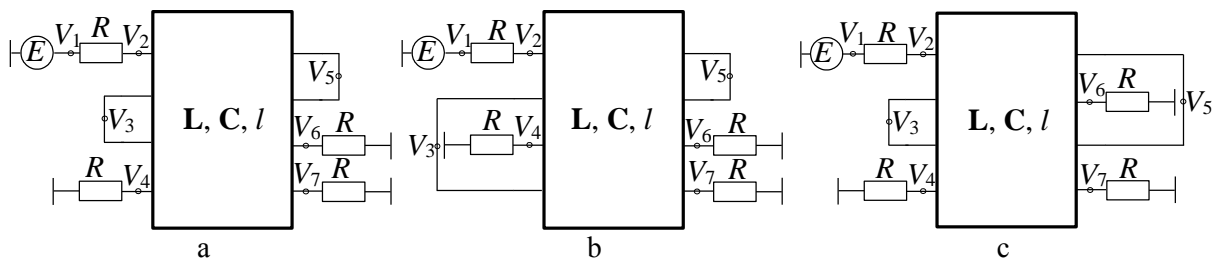


**Figure 2.** Schematic diagrams of half-turns connection: 1 (a), 2 (b) and 3 (c).

The construction of a cross-sectional geometric model with optimal values of the parameters ( $s=510 \mu\text{m}$ ,  $w=1600 \mu\text{m}$ ,  $t=18 \mu\text{m}$ ,  $h=500 \mu\text{m}$ ,  $\epsilon_r=4,5$ ), the calculation of matrices of per-unit-length coefficients of electrostatic ( $C$ ) and electromagnetic ( $L$ ) inductions, the drawing up of a diagram for simulation, the assignment of terminations and excitation, as well as the calculation of the time response, were made similarly to the simulation of structures of 4 cascaded half-turns [5] in the TALGAT software [6], selected due to its acceptable accuracy and low computational costs [7].

### 3. Simulation results

The time responses at the output of the structures under study for  $l=1 \text{ m}$  (nodes  $V_6$  in Figure 2 a and 2 c and  $V_7$  in Figure 2 b) are presented in Figure 3.

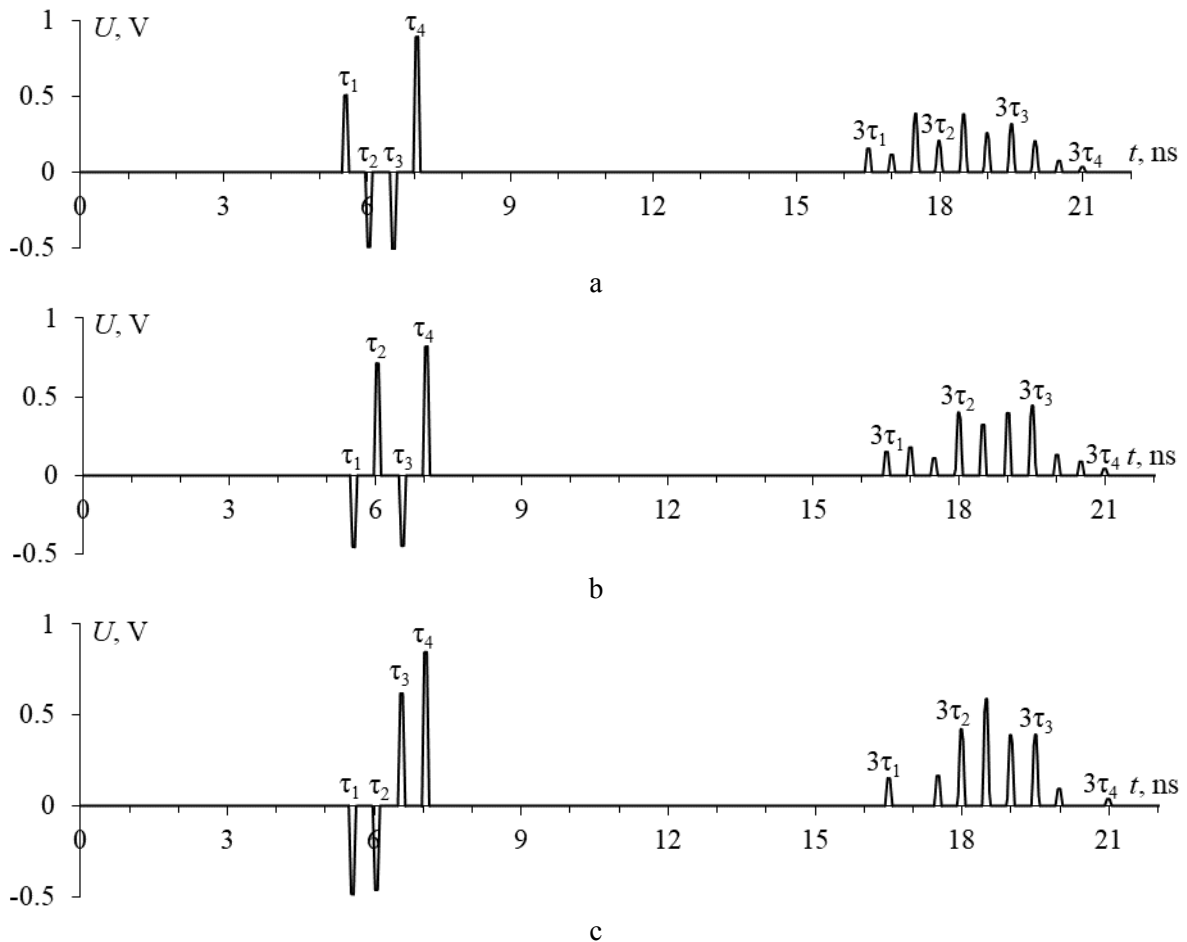


**Figure 3.** Voltage waveforms at the output of diagrams 1 (a), 2 (b) and 3 (c) for  $l=1$  m.

Figure 3 shows two groups of pulses. Their time delays are multiples of 1 and 3 per-unit-lengths delays, respectively. Let us consider them separately.

In the first group, a pair of pulses with negative polarity is observed. The same pulses were observed when simulating the reflection symmetric ML of 4 half-turns [5]. However, when simulating the reflection symmetric MF, such pulses were not observed. Figure 3 shows that the maximum voltage at the end of the active conductor is determined by the amplitude of the pulse from the first group with a delay of  $\tau_4$  and is equal to 0.88 V for diagram 1, 0.81 V for diagram 2 and 0.84 V for diagram 3. Meanwhile, the amplitude of the output voltage in the structure of 4 half-turns (0.88 V) is similarly determined by the amplitude of the pulse from the first group.

In the second group of pulses, it is noteworthy that, in addition to the main pulses with delays being multiple of per-unit-length delays of the modes, there exist six (for diagrams 1 and 2) and four (for diagram 3) additional pulses with different delay values. A detailed analysis of their waveforms shows that they are different from the trapezoid, which indicates possible overlapping of neighboring pulses. Therefore, the actual number of additional pulses may be more than those obtained during simulation. In addition, this is confirmed by an increase in the total amplitude of some additional pulses. To perform additional verification of this assumption, let us change the  $l$  value from 1 to 8 m for all diagrams. The fragments of the output voltage waveforms with pulses whose delays are equal to 24 mode delays are presented in Figure 4.

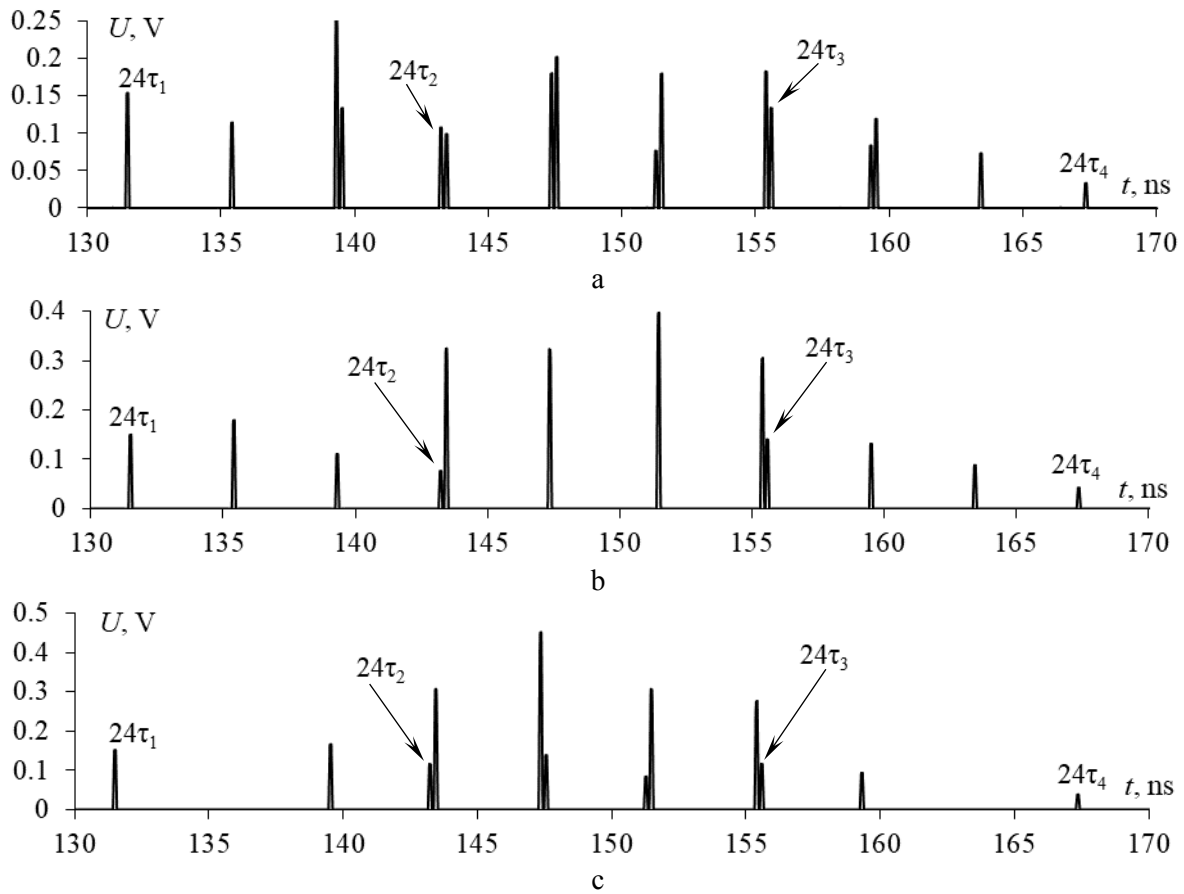


**Figure 4.** Voltage waveforms at the output of diagrams 1 (a), 2 (b) and 3 (c) for  $l=8$  m.

The simulation results confirm the presence of a larger number of additional pulses in the diagrams under investigation. Their values increased from 6 (for diagrams 1 and 2) and 4 (for diagram 3) to 12 (for diagram 1) and 8 (for diagram 2) and 6 (for 3). Meanwhile, for diagrams 2 and 3, it was not possible to significantly increase the time intervals between pulses by increasing the line length. The voltage amplitude at the output of these diagrams is higher than that of diagram 1, which indicates overlapping of some pulses and, as a consequence, an increase in the total amplitude. On this basis, for diagrams 2 and 3, the value of  $h$  was increased from 0.5 mm to 1 mm to increase the time intervals between decomposition pulses. The voltage waveforms at the output of diagrams 2 and 3 are shown in Figure 5.

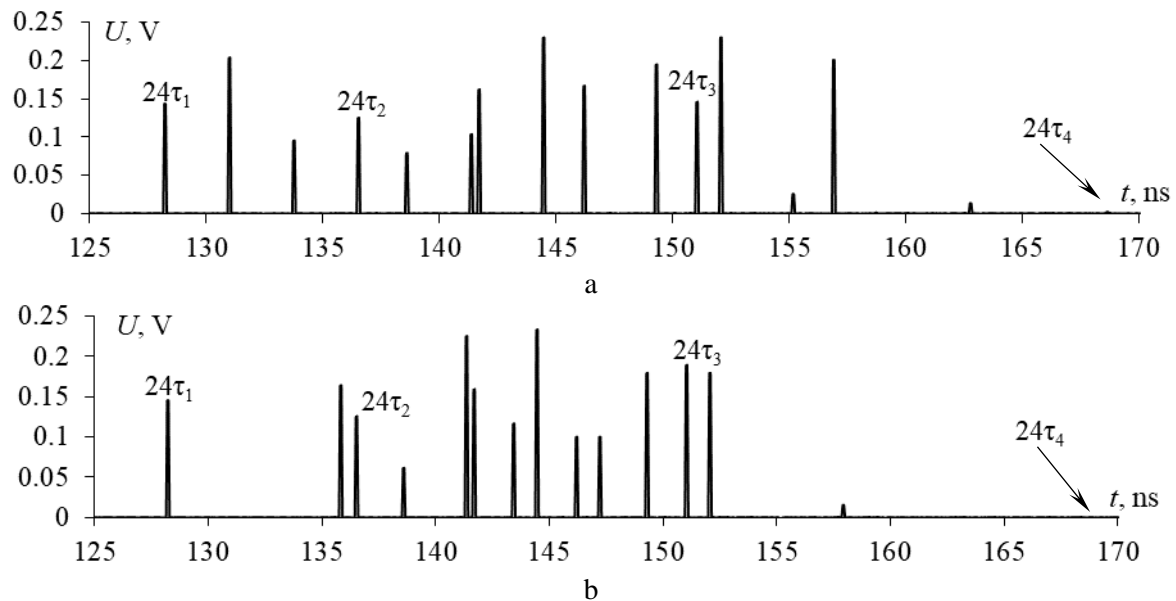


**Figure 5.** Voltage waveforms at the output of diagrams 2 (a) and 3 (b) for  $h=1$  mm and  $l=8$  m.

Figure 5 shows the decomposition of all pulses in diagrams 2 and 3. The number of additional pulses, similar to diagram 1, is equal to 12 for each diagram. Table I shows the delay values of all pulses 16 in total multiplied by 24 for  $h=0.5$  mm for diagram 1 and  $h=1$  mm for diagrams 2 and 3 for  $l=8$  m.

**Table 1.** Delays (ns) of pulses 1–16 for diagrams 1, 2 and 3.

№	1	2	3	4	5	6	7	8	9	10	11	12	13	14	15	16
1	131.4	135.3	139.2	139.4	143.1	143.3	147.2	147.4	151.1	155.3	155.3	155.5	159.2	159.4	163.3	167.2
2	128.1	130.9	133.6	136.4	138.5	141.2	141.6	144.3	146.1	149.2	150.96	151.96	155.0	156.8	162.7	168.5
3	128.1	135.7	136.4	138.5	141.2	141.6	143.3	144.3	146.1	147.1	149.2	150.9	151.9	155.0	157.8	168.5

For 4 half-turns [5], it was found that the delays of additional pulses are equal to the arithmetic mean of the two per-unit-length delays of modes 1–4 in different variants. However, this statement is not suitable for the reflection symmetric ML of 3 half-turns. Meanwhile, analyzing Figures 4–5 and Table I, it can be expected that the delays of each of the additional pulses are equal to the arithmetic mean value of the delays of two pulses, both main and additional. Let us consider in detail this statement for diagram 1. The assumed delays of additional pulses at  $l=8$  m and  $h=0.5$  mm are presented in Table II.

**Table 2.** The estimated values of additional pulse delays being equal to the arithmetic mean (AM) value of two delays of modes 1–4 for diagram 1.

AM	$(24\tau_1+24\tau_2)/2$	$(24\tau_1+24\tau_3)/2$	$(24\tau_2+24\tau_3)/2$	$(24\tau_1+24\tau_4)/2$	$(24\tau_2+24\tau_4)/2$	$(24\tau_3+24\tau_4)/2$
$t$ , ns	137.287	143.467	149.333	149.353	161.4	155.219

In Figure 4 a, there are no pulses with delay values from Table II. However, a detailed analysis of Figure 4 a showed that the delay values of each additional pulse are equal to the arithmetic mean of the delay values of the other two pulses. The delay of pulse 2 is equal to the arithmetic mean value of the delays of pulses 1 and 3; pulse 3 – 2 and 5; pulse 4 – 1 and 8; pulse 6 – 3 and 8; pulse 7 – 5 and 10; pulse 8 – 4 and 12; pulse 9 – 5 and 13; pulse 10 – 8 and 11; pulse 11 – 9 and 14; pulse 13 – 9 and 16; pulse 14 – 12 and 15; pulse 15 – 14 and 16. Pulses 1, 5, 12 and 16 are the main ones.

#### 4. Conclusion

Thus, the possibility of USP decomposition in a reflection-symmetric ML of three cascaded half-turns is shown. When simulating the time response in 3 considered diagrams, additional pulses were detected in the output signal. Depending on the way how conductors are connected, the additional pulses have delay values that are equal to the arithmetic mean value of the two pulse delays, both main and additional.

It is shown that the output voltage amplitude of the reflection-symmetric ML for all diagrams is determined by the amplitude of the pulse from the first group with a delay of  $\tau_4$ . Meanwhile, it can be assumed that when optimizing the reflection symmetric ML according to the criterion of equalizing the time intervals between decomposition pulses, including additional ones, in these circuits it is possible to increase USP attenuation. It is noteworthy that to implement such circuit not 6 but only 2 resistors at the ends of passive conductors will be required. Moreover, unlike the structure of 4 half-turns [5], the input and output are at different ends of the structure, which can be useful in practical application. In the future, we plan using analytical expressions that describe additional pulses in the time domain, as well as to reveal the nature of additional impulses in such structures.

#### 5. Acknowledgments

The reported study was funded by Russian Science Foundation (project №19-19-00424).

#### References

- [1] Radasky W A, Baum C E and Wik M W 2004 *Special issue of IEEE Transactions on Electromagnetic Comconspatibility* **46(3)** 314–21
- [2] Gizatullin Z M and Gizatullin R M 2016 *Journal of Communications Technology and Electronics* **61(5)** 546–50
- [3] Mora N, Vega F, Lugrin G, Rachidi F and Rubinstein M 2014 *System and assessment notes* **41** 1–93
- [4] Gazizov A T, Zabolotsky A M and Gazizov T R 2016 *IEEE Transactions on Electromagnetic Compatibility* **58(4)** 1136–42
- [5] Chernikova E B, Belousov A O and Gazizov T R 2019 *IOP Conf. Series: Materials Science and Engineering* **597** 1–6
- [6] Kuksenko S P 2019 *IOP Conf. Series: Materials Science and Engineering* **560** 1–7
- [7] Orlov P E and Buichkin E N *18th Int. conf. on micro/nanotechnologies and electron devices (EDM-2017)* pp 54–8